Long Mean Free Path of Hot Electrons Selectively Injected to Higher Subbands

B. Laikhtman, U. Sivan, A. Yacoby, C. P. Umbach, M. Heiblum, J. A. Kash, and H. Shtrikman
IBM Research Division, Thomas J. Watson Research Center, Yorktown Heights, New York 10598
(Received 27 June 1990)

The long hot-electron mean free path observed by Sivan, Heiblum, and Umbach in high-mobility 2D electron-gas heterostructures is explained by electron transport in the second subband. Our estimates show that the mean free path in the second subband is longer by 2 orders of magnitude than that in the first subband. New magnetic-focusing measurements reveal hot-electron velocities lower than the Fermi velocity, as expected for a higher-subband transport. The electrostatic potential near a biased constriction used as the hot-electron injector is shown to induce nonadiabatic intersubband transfer.

PACS numbers: 73.20.Dx, 73.50.Bk, 73.50.Gr

Recently, Sivan, Heiblum, and Umbach[1] reported on a study of hot-electron transport over distances shorter than the elastic mean free path (mfp) in a high-mobility two-dimensional electron gas (2DEG). In that experiment, hot electrons were injected from a point contact electrostatically defined using two metallic gates deposited on top of the structure and detected by a similar point contact, 2 μm away, which served as an energy spectrometer. For electrons injected at energies above the longitudinal-optical- (LO-) phonon energy (36 meV in GaAs), LO-phonon emission was observed, along with a very short mfp, as expected theoretically. However, for injection energies below 36 meV, a surprisingly long mfp, of the order of 2 μm, was found. The measured mfp was roughly an order of magnitude longer than expected theoretically for electron-hole (in the conduction band) excitations[2,3] and about 30 times longer than the mfp for electron-plasmon scattering[2,3] expected theoretically and found in optical experiments in GaAs quantum wells[4] and bulk GaAs.[5] This apparent discrepancy between theory and experiment[1] is the subject of the present work. We show that the discrepancy vanishes if the detected electrons traveled in the second subband of the 2DEG rather than in the first one. We explain why hot electrons in higher subbands are expected to have a longer mfp and how the electron transfer to the higher subband can occur. Finally, we provide experimental evidence for such unconventional transport.

The primary inelastic-scattering mechanisms for hot electrons in a 2DEG are expected to be electron-hole pair excitations in the conduction band and, above some energy thresholds, electron-plasmon and LO-phonon scattering. The mutual interaction between hot electrons traveling in higher subbands, and cold ones in the lowest one, is modified in the following three ways. First, due to the relatively extended nature of the wave functions corresponding to higher subbands of an accumulation layer, the spatial overlap of the hot and the cold electrons is substantially reduced. Second, the threshold energy for plasmon emission is shifted by the subband separation (in an accumulation layer the probability of scattering from an upper subband to the lowest one is negligibly small), and third, for low-energy electrons in the higher subbands, the phase space for scattering is reduced. Our calculations of the Coulomb interaction matrix elements for a process in which none of the electrons change subband[6] yield, for n-type unintentional residual doping (which is the case in both Ref. 1 and the experiment reported below), a matrix element which is approximately 5 times smaller than the intraband one. Since the scattering rate is proportional to the matrix element squared, the mfp of second-subband electrons is at least 25 times longer than that of electrons with the same kinetic energy in the first subband. Numerical calculations by Artaki and Hess[7] show an even larger reduction of the electron-hole excitation rate (by an additional factor of 4). For the experiment reported in Ref. 1, with $E_F=7$ meV and $E-E_F=35$ meV (just below the LO-phonon emission threshold), theory[2,3] predicts a mfp of ≈ 1000 Å for electrons in the first subband due to electron-hole excitation. The projected mfp for second-subband transport should therefore exceed the lower bound found in the experiment in Ref. 1. The same arguments hold for plasmon emission. For the same parameters, the mfp in the first subband is estimated to be ≈ 300 Å (provided the threshold for plasmon emission is being exceeded), leading to a projected mfp for hot electrons in the second subband comparable with the device's dimensions. For a large subband separation the threshold is shifted above the LO-phonon energy.

Our novel explanation for the long, experimentally observed, mfp requires some mechanism for electron transfer to higher subbands. The accepted point of view, clearly formulated by Glazman *et al.*,[8] is that the injected electrons propagate through a point-contact injector adiabatically; i.e., they do not change their discrete quantum numbers. Here we argue that this is far from being the case for hot electrons injected from a strongly biased constriction.

The generic hot-electron injector used in both Ref. 1 and the experiment presented here consisted of two metallic gates [see emitter (E) in Fig. 1] deposited on the surface of the heterostructure. The typical separation between the gates was 200–400 nm and their minimum

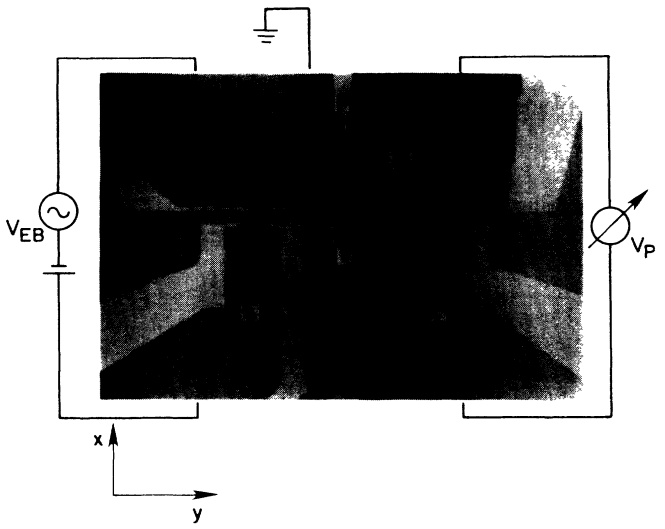

FIG. 1. A top-view micrograph of one of the devices used in the magnetic-focusing experiment. The light areas are the metallic gates deposited on top of the GaAs-AlGaAs heterostructure.

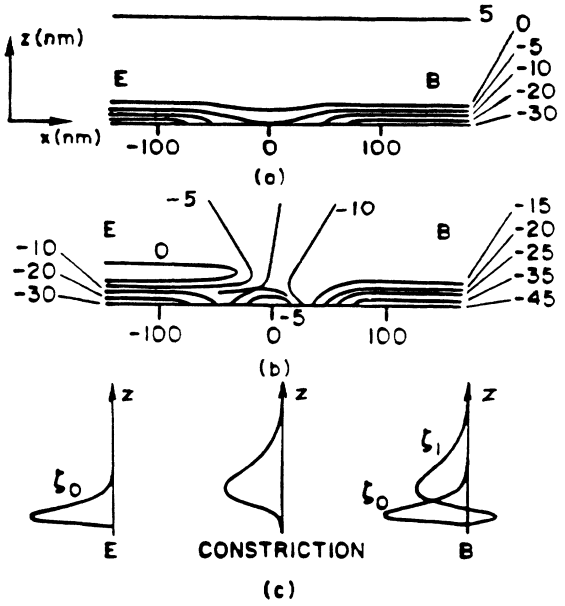

FIG. 2. Electrostatic energy and electron wave functions near a constriction in a 2DEG with n-type unintentional background doping (schematic). The AlGaAs barrier layer is at $z<0$. (a) Equipotential lines for $V_{EB}=0$. The numbers show the electrostatic energy in meV relative to the Fermi energy. (b) The same picture for $|V_{EB}|=15$ mV. (c) The electron wave functions of the first (ζ_0) and the second (ζ_1) subbands in various regions.

widths were usually 50–100 nm. An application of a high enough negative voltage to the gates (relative to the 2DEG) confined the electrons to the ungated regions only. Hot electrons were injected by negatively biasing, with V_{EB}, the 2DEG on the emitter side of the constriction relative to the base side. The resulting electrostatic-energy map[6] in the plane $y=0$ perpendicular to the plane of the 2DEG (x-y plane) is schematically depicted in Fig. 2(a) for $V_{EB}=0$. The lines designate equipotential lines and energy is measured relative to E_F. The line $z=0$ marks the interface between the GaAs ($z>0$) and AlGaAs ($z<0$) regions and the line $x=0$ coincides with the constriction's center. Far from the center of the constriction the electrostatic energy $\Phi(x,z)\simeq\Phi(z)$ does not depend on the gate potential. Near the center the energy is determined by the intrinsic field due to the doping in the AlGaAs barrier, the field induced by the gates, and the unintentional doping in the nominally undoped GaAs layer.

The electrostatic map is substantially modified by application of a biasing voltage across the constriction. A schematic energy map is presented in Fig. 2(b) for $|V_{EB}|=15$ mV. Far from the center of the constriction and close enough to the heterointerface, the shape of the potential is similar to that in Fig. 2(a), but it is shifted by the external bias eV_{EB}. Further away from the heterointerface the electrostatic energy approaches the solution of Laplace's equation with boundary conditions $\Phi=0$ for $x<0$, $z=0$ and $\Phi=eV_{EB}$ for $x>0$, $z=0$, which is $\Phi=eV_{EB}(1-\theta/\pi)$, where $\tan\theta=z/x$. Two features of the potential in Fig. 2(b) are important for the intersubband transfer. The first is a depletion of the 2DEG and a very shallow potential well near the center of the constriction leading to a greater extension of the wave function in the z direction compared with the wave function far from the constriction. In an accumulation layer with electron concentration of 2×10^{11} cm^{-2} (Ref. 1) the first-subband wave function is extended in the z direction for about 200 Å. Thus, the extension of the wave function in the constriction is of the order of the characteristic size of the opening (about 0.1 μm). Consequently, upon applying V_{EB}, the condition for adiabatic propagation, namely, that the size of the wave function be small compared to the length scale of the potential change in the x and y directions, is violated. The second feature to note is related to the fact that the potential near the constriction is controlled by the gate potential and is not significantly affected by a bias voltage V_{EB} applied to the 2DEG. As a result, a potential saddle point on the path from the emitter to the base is created, and shifts away from the interface as V_{EB} is further increased. This potential shifts the "center of gravity" of the wave function away from the interface [Fig. 2(c)]. Eventually, the spatial overlap of this wave function with the second-subband wave function in the base becomes larger than the overlap with the wave function of the first subband. This, along with the nonadiabatic propagation, leads to a preferential injection to the second subband in the base. Transfer to even higher subbands is also conceivable. Note that in the discussion of the potential landscape of Fig. 2 we implied n-type residual doping. The results, however, are also qualitatively applicable to

samples with p-type residual doping, although the characteristic parameters can be quite different.

In order to test these ideas we have performed a series of magnetic-focusing[9] experiments in which the electronic velocity in the base region was measured as a function of injection energy. A top-view micrograph of one of the devices is shown in Fig. 1. The light areas are metallic gates patterned on top of the GaAs-AlGaAs heterostructure containing the 2DEG. One pair of gates was utilized as a hot-electron injector (E in Fig. 1) and a second pair was used as a voltage probe (P) to measure the local chemical potential near its opening. The other gates (T) and (F) were used to verify the correspondence between trajectories and different peaks in measurements of the probe voltage V_P versus the applied magnetic field B (see below). The distance between the two openings varied between 1 and 3 μm in different devices. The E, P, and B regions of the 2DEG were contacted using NiGeAu-alloyed Ohmic contacts. The data presented below were measured at 4.2 K in an illuminated sample with carrier concentration of 4.7×10^{11} cm^{-2} ($E_F=16.7$ meV) and mobility of 1.3×10^6 cm^2/V sec. Similar results were obtained in a nonilluminated sample with expected modification due to the somewhat lower E_F and mobility.

Four characteristic curves of V_P versus magnetic field at different injection energies are shown in Fig. 3 (gate F grounded). At low biasing voltages, $|V_{EB}|\leq 5$ meV, the various peaks shifted monotonically, as expected, with V_{EB}, and the kinetic energy calculated from the magnetic field corresponding to their position,

$$E=(eBL)^2/2mi^2, \quad (1)$$

varied linearly with the applied dc bias.[9] Here, L is the distance between the centers of E and P, m is the effective mass, and i is the peak number. When V_{EB} was increased to -6 mV, a new set of peaks appeared at 950 and 1800 G while the original peak amplitude was considerably reduced. For even larger V_{EB} (e.g., -9 mV in Fig. 3), the new set of peaks became more pronounced while the original one disappeared altogether. We interpret the first two peaks of the new set as a result of second-subband (or higher-subband) trajectories with 0 and 1 bounces from the center T. The third peak in Fig. 3 can be energetically interpreted as resulting from either a second-subband trajectory with two bounces or a first-subband trajectory with one bounce.

The variation of the measured kinetic energy is depicted in Fig. 4 as a function of eV_{EB}. For $|V_{EB}|\leq 5$ meV, the deduced energy varied linearly with the applied bias, $E\simeq E_F+0.82eV_{EB}$. A comparable coefficient, 0.68, was obtained by Williamson *et al.*,[9] where the deviation from a unity prefactor was attributed to series resistances associated with the Ohmic contacts. We, however, interpret this result differently and attribute the deviations from the ideal case (unity coefficient) to electronic drift in the presence of crossed magnetic and electric fields, where the latter is induced by the biased gates. Assuming, for instance, an electrostatic barrier $\Delta\Phi=10$ meV, a potential spread away from the gate along the y direction to $a=2000$ Å, and $B=1000$ G, a drift velocity parallel to the gate $v_D=\Delta\Phi/eaB\simeq5\times10^7$ cm/sec is obtained. Since this velocity is twice as large as the Fermi velocity, it is apparent that drift motion plays an important role in magnetic-focusing experiments in a 2DEG. Numerical simulations carried out on model potentials have yielded a comparable coefficient relating the kinetic energy and the injection voltage. The effect of the drift becomes

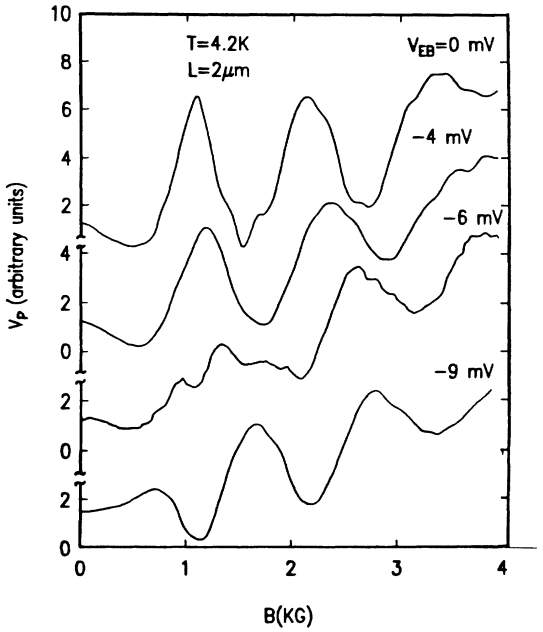

FIG. 3. The measured voltage V_P as a function of magnetic field for different bias voltages V_{EB}. Notice the appearance of a new set of peaks for $|V_{EB}|\gtrsim 6$ mV.

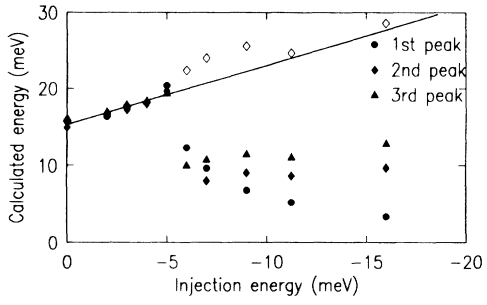

FIG. 4. The electron kinetic energy as a function of the injection energy calculated from Eq. (1). The solid triangles and open diamonds correspond to different interpretations of the peak around 2.5 kG: the third peak of the second subband and the second peak of the first subband, respectively.

even more predominant for second-subband transport where the kinetic energy of the electrons is smaller. In that case, the peaks in V_P vs B are expected to shift more slowly with injection energy and given a long enough potential tail might even reverse their trend. The negative slope of the energy, calculated according to the simple model corresponding to Eq. (1), versus injection energy for the second set of peaks is clearly seen in Fig. 4. Analytical and numerical simulations also give the observed trend, though the substantial decrease in the kinetic energy deduced from the experiment cannot be fully accounted for assuming realistic potential tails. As mentioned earlier, the third peak for $|V_{EB}| \geq 5$ mV can be marginally interpreted as the second peak due to first-subband transport. This interpretation is depicted in Fig. 4 by open diamonds. Substituting the experimental results for the new set of peaks into Eq. (1) leads to an electronic velocity considerably smaller than v_F (for all values of V_{EB}), thus strongly supporting our higher-subband transport picture.

To check our association of a given peak in Fig. 3 with a corresponding trajectory, we used the gates F and T. As expected, upon applying large enough negative voltage to F, the first peak associated with either the first set ($|V_{EB}| \leq 5$ meV) or the second one ($|V_{EB}| > 5$ meV) was eliminated with practically no effect on higher-order peaks. Note, however, that a somewhat more negative gate voltage was necessary to eliminate the first peak of the second set, suggesting that the corresponding trajectory was passing closer to the gate T. Such a behavior is expected for cases where the drift velocity plays an important role. Similarly, upon grounding T, all higher-order peaks, corresponding to bouncing trajectories, were eliminated in both sets. We may thus conclude that the new set of peaks corresponds to trajectories similar to those of the first subband.

The kinetic energy measured from the second set of peaks implies a first to second-subband separation of roughly 10–15 meV. This relatively small value is expected in a 2DEG with n-type unintentional background doping. To check this conclusion we have measured the subband energy separation by resonant electronic Raman backscattering in the $z(xy)\bar{z}$ geometry (the incident light with polarization along x propagated along the z direction and backscattered light with polarization along y was measured). The measurements have been done at $T=2$ K on material from the same wafer using a sample without gates and contacts. A subband splitting of 14.8 ± 0.3 meV was measured, consistent with our determination of that quantity from the magnetic-focusing measurements.

The measured subband separation implies that injection to the second subband is energetically possible even for a very small V_{EB}. Yet, it is apparent from Figs. 3 and 4 that magnetic-focusing peaks due to second-subband transport appeared only for $|V_{EB}| \geq 5$ mV. This observation is in line with the explanation given above emphasizing the necessity of some critical bias for effective interband transfer.

In summary, we have shown that the experimentally observed long mfp of hot electrons in a high-mobility 2DEG (Ref. 1) can result from hot-electron transport in the second subband. Our model is supported by new hot-electron magnetic-focusing experiments where an electron velocity lower than the Fermi velocity was observed. We described the electrostatic potential profile in the vicinity of a biased point contact induced in a 2DEG and argued that electrons should preferably be injected from the lowest subband in the emitter to a higher subband in the base.

One of us (B.L.) is grateful to T. Theis who attracted his attention to the problem of a long mfp in Ref. 1 and advised keeping in mind a many-subband picture in dealing with transport in a 2DEG. One of us (U.S.) was partially supported by the Weizmann Foundation.

Note added.—Recently, we have realized that some of the features in the present experiment can also result from the modulation of the constriction by the applied ac voltage. However, other features contradict this possibility and further experiments are needed to separate this effect from the one discussed in the Letter.

[1]U. Sivan, M. Heiblum, and C. P. Umbach, Phys. Rev. Lett. **63**, 992 (1989).

[2]P. Hawrylak, G. Eliasson, and J. J. Quinn, Phys. Rev. B **37**, 10187 (1988).

[3]R. Jalabert and S. Das Sarma, Phys. Rev. B **40**, 9723 (1989).

[4]W. H. Knox, D. S. Chemla, and G. Livescu, Solid State Electron. **31**, 425 (1988).

[5]J. A. Kash, Phys. Rev. B **40**, 3455 (1989).

[6]We are indebted to F. Stern for the self-consistent calculation of the potential and electron wave functions in an ideal 2DEG.

[7]M. Artaki and K. Hess, Solid State Electron. **31**, 383 (1988); Phys. Rev. B **37**, 2933 (1988).

[8]L. I. Glazman, G. B. Lesovik, D. E. Khmel'nitskii, and R. I. Shekhter, Pis'ma Zh. Eksp. Teor. Fiz. **48**, 218 (1988) [JETP Lett. **48**, 238 (1988)].

[9]J. G. Williamson, H. van Houten, C. W. J. Beenakker, M. E. I. Broekaart, L. I. A. Spendeler, B. J. van Wees, and C. T. Foxon, Phys. Rev. B **41**, 1207 (1990).

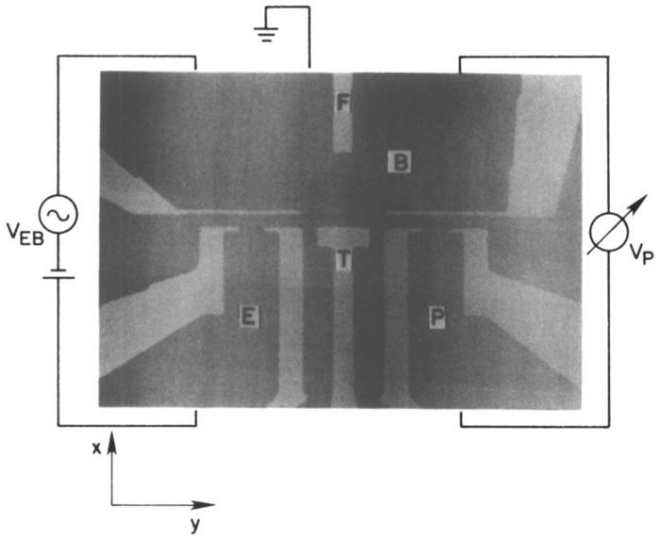

FIG. 1. A top-view micrograph of one of the devices used in the magnetic-focusing experiment. The light areas are the metallic gates deposited on top of the GaAs-AlGaAs heterostructure.